Investigation of Crystalline Phases in the α-Fe₂O₃/α-Al₂O₃ System*

Mira Ristić,[a,] Stanko Popović,[b] and Svetozar Musić[a]**

[a]*Division of Materials Chemistry, Ruđer Bošković Institute, P. O. Box 180, HR-10002 Zagreb, Croatia*
[b]*Department of Physics, Faculty of Science, P.O. Box 331, HR-10002 Zagreb, Croatia*

Abstract. Mixtures containing the desired weight ratios of α-Fe$_2$O$_3$ and γ-AlOOH were homogenized in the planetary mill, then pressed into tablets and heated up to 1200 °C. All samples were characterized by X-ray diffraction, Mössbauer spectroscopy, Field emission scanning electron microscopy and Energy dispersive X-ray analysis. Two types of solid solutions of general formula α-(Al$_x$Fe$_{1-x}$)$_2$O$_3$ were found; one solid solution was closely related to α-Fe$_2$O$_3$, the other to α-Al$_2$O$_3$. The terminal solid solubility limits, $r = 27.0 \pm 0.5$ mole ratio of α-Al$_2$O$_3$ in α-Fe$_2$O$_3$ and $r = 9.0 \pm 0.5$ of α-Fe$_2$O$_3$ in α-Al$_2$O$_3$, were determined. The Mössbauer spectra showed a broadening of spectral lines and a decrease in the hyperfine magnetic field of α-Fe$_2$O$_3$ with incorporation of Al^{3+} ions in the α-Fe$_2$O$_3$ structure. For mole fractions between $x = 0.40$ and 0.70, the Mössbauer spectra were considered as the superposition of a sextet and quadrupole doublet(s). In this concentration range the samples showed an almost constant value of hyperfine magnetic field. For $x = 0.90$ and 0.93, the Mössbauer spectra were considered as a superposition of two quadrupole doublets, whereas for $x = 0.95$ the superposition of two quadrupole doublets and one singlet was considered. The origin of this singlet with the isomer shift close to zero is not clearly understood. FE-SEM showed a strong sintering effect on the particles in all samples in the α-(Al$_x$Fe$_{1-x}$)$_2$O$_3$ system.

Keywords: solid solutions, α-Fe$_2$O$_3$, α-Al$_2$O$_3$, XRD, ^{57}Fe Mössbauer, FE-SEM, EDS

INTRODUCTION

α-Al$_2$O$_3$ (corundum) and α-Fe$_2$O$_3$ (hematite) belong to the same space group, *R3c* (No. 167). The latticeconstants at 25 °C, in terms of hexagonal axes are: $a = 0.4758$ and $c = 1.2991$ nm for α-Al$_2$O$_3$; $a = 0.5034$ and $c = 1.3752$ nm for α-Fe$_2$O$_3$.[1] The differences in *a* and *c* parameters, 5.80 and 5.86 %, respectively, are a consequence of different ionic radii of the metals (for coordination six): 0.054 nm for Al^{3+} and 0.065 nm for Fe^{3+}.

Al^{3+}-substituted α-Fe$_2$O$_3$ and Fe^{3+}-substituted α-Al$_2$O$_3$ have been frequently investigated because of their interesting properties from the academic point of view on the one hand, and because of their importance in various environmental systems (soils and sediments) and industrial processes (bauxite mining, production of various ceramics) on the other hand.

Brown *et al.*[2] measured the lattice parameters for α-Al$_2$O$_3$ samples containing Fe^{3+} ions and found a linear increase in the *a* parameters with an increase in α-Fe$_2$O$_3$ up to $r = 10.5$. De Grave *et al.*[3] prepared a series of aluminium substituted hematites, α-(Al$_x$Fe$_{1-x}$)$_2$O$_3$ with *x* up to 0.32 by heating aluminium substituted goethites at 500 or 900 °C. The particles obtained at 500 °C were $\approx$ 20–100 nm in size. With an increase in the heating temperature up to 900 °C, the fraction *x* decreased to $\approx$ 0.15. Wolska and Szajda[4] heated Al(OH)$_3$ / Fe(OH)$_3$ coprecipitates up to 900 °C and noticed the formation of solid solutions up to $x = 0.15$. Cordier *et al.*[5] investigated the formation of α-Al$_{1.8}$Fe$_{0.2}$O$_3$ solid solution from the precursors obtained by the combustion method. Citric acid or urea or a mixture of both as fuel were used varying the fuel/nitrate ratio.

The α-Fe$_2$O$_3$ / α-Al$_2$O$_3$ powders were subjected to high-energy ball-milling varying the mechanochemical conditions such as the time of milling and the milling medium (vial and balls).[6–9] A strong effect of the mil-

---

* Dedicated to Professor Emeritus Drago Grdenić, Fellow of the Croatian Academy of Sciences and Arts, on the occasion of his 90th birthday.
** Author to whom correspondence should be addressed. (E-mail: ristic@irb.hr)

ling medium on the final phase composition of the powders was observed. Apart from the solid solutions of α-type, the formation of α-Fe and $FeAl_2O_4$ was observed. α-Fe and $FeAl_2O_4$ can be considered contaminants due to the wear of the milling medium (vial and balls).

Kákoš *et al.*[10] found a strong effect of Fe^{3+} ions on the crystallization of α-Al_2O_3 from boehmite gel which contained Fe^{3+} ions at the start of the calcination process. Stösser *et al.*[11] investigated the role of Fe^{3+} ions on the transformation from boehmite or pseudoboehmite xerogels via transition aluminas to corundum. The authors concluded that the decrease in the temperature of α-Al_2O_3 formation is due to the action of fine α-Fe_2O_3 particles. Isolated Fe^{3+} ions had almost no influence on the temperature of Al_2O_3 formation. Liu *et al.*[12] investigated the α-Fe_2O_3/α-Al_2O_3 system combining the sol-gel method and the thermal treatment of the precursors obtained. $\gamma \rightarrow \alpha$-$Al_2O_3$ transformation proceeded at lower temperatures due to α-Fe_2O_3 doping. Zhang *et al.*[13] investigated the interaction of iron oxide coatings and submicrospherical alumina. The effects such as the separation of iron oxide particles upon heating at high temperature, the hindering of γ-Fe_2O_3 to α-Fe_2O_3 transformation at temperatures higher than 700 °C, and the formation of solid solutions were observed. These effects were also linked to the amorphous or crystalline properties of the substrate. Evidently, the properties of the mixed α-Fe_2O_3/α-Al_2O_3 system are highly dependent on the experimental conditions prevailing in sample preparation.

As a follow-up to previous work[14] we have further investigated the properties of the α-Fe_2O_3/α-Al_2O_3 system using ^{57}Fe Mössbauer spectroscopy, FE-SEM and EDS techniques, with the aim to obtain more information about this mixed oxide system.

EXPERIMENTAL

Sample Preparation

γ-AlOOH (boehmite) and α-Fe_2O_3 of analytical purity were used as starting chemicals. A series of mixtures of these two compounds containing the desired weight ratios were mechanically mixed for 1 hour using a planetary mill by Fritsch (Pulverissete 5). Agate bowl and balls (99.9 % SiO_2) were used. The use of this milling medium minimizes the contamination of a mixed oxide system. In systematic investigations Štefanić *et al.*[15,16] showed what a strong effect of wearing products on the properties of ZrO_2 can occur during the milling process. After milling the powders were pressed into tablets, then heated. For temperatures above 1000 °C, the LKO II furnace with Kanthal heaters was used. The

samples were heated step by step as follows: 200 °C for 1 h, 300 °C for 1 h, 400 °C for 1 h, 600 °C for 1 h, 900 °C for 3 h and 1200 °C for 2 h. After heating at 1200 °C the samples were cooled in the furnace to $\approx$ 300 °C, then taken out from the LKO II furnace and further cooled to room temperature (RT). The calcined tabletes were ground, then characterized with instrumental techniques.

Instrumentation

X-ray powder diffraction measurements were carried out at 25 °C with a Philips diffractometer, model MPD 1880. The lattice parameters of α-Al_2O_3 and α-Fe_2O_3, measured as in the present work, were practically equal to reference values, and for that reason our data were used for calibration of the angular scale of the diffractometer.

The ^{57}Fe Mössbauer spectra were recorded at 20 °C in the transmission mode using the configuration by WissEl GmbH (Stanberg, Germany). The ^{57}Co in the rhodium matrix was used as a Mössbauer source. Velocity scale was calibrated with α-Fe foil at 20 °C. Isomer shifts, δ, are given relative to α-Fe at 20 °C. 1024 channels were used to record the Mössbauer spectra, then the spectra were folded. The folded Mössbauer spectra were fitted using the MossWinn program.

The samples were also inspected using a thermal FE-SEM (model JSM-7000F), manufactured by *JEOL Ltd.* The FE-SEM was linked to an EDS/INCA 350 (energy dispersive X-ray analyzer) manufactured by *Oxford Instruments Ltd.* The specimens were not coated with an electrically conductive surface layer.

RESULTS AND DISCUSSION

XRD Results

The results of XRD phase analysis are given in Table 1. In the same table nominal fractions of Al_2O_3 are also given. The formation of two types of solid solutions of the form α-$(Al_xFe_{1-x})_2O_3$ was observed. For $0 \leq x \leq 0.91$, a terminal solid solution phase, F, closely related to α-Fe_2O_3, and for $0.27 \leq x \leq 1$ a terminal solid solution phase, A, closely related to α-Al_2O_3, were present. A schematic representation of the Bragg angles and relative intensities (radiation Cu $K\alpha_1$) of the prominent diffraction lines, 214 and 300, of phases A and F for $x = 0$, 0.30, 0.70 , 0.90 and 1 are shown in Figure 1a. The variation of the Bragg angle (Cu $K\alpha_1$) of diffraction lines 214 and 300 of phases A and F with x is shown in Figure 1b. In the single phase regions, the lattice constants a and c of both phases F and A decreased as x increased. In the two-phase region ($0.27 \leq x \leq 0.91$) the lattice constants a and c of both phases did not change,

Table 1. X-ray powder diffraction analysis of samples prepared in the α-$(Al_xFe_{1-x})_2O_3$ system; phase A is closely related to α-Al_2O_3
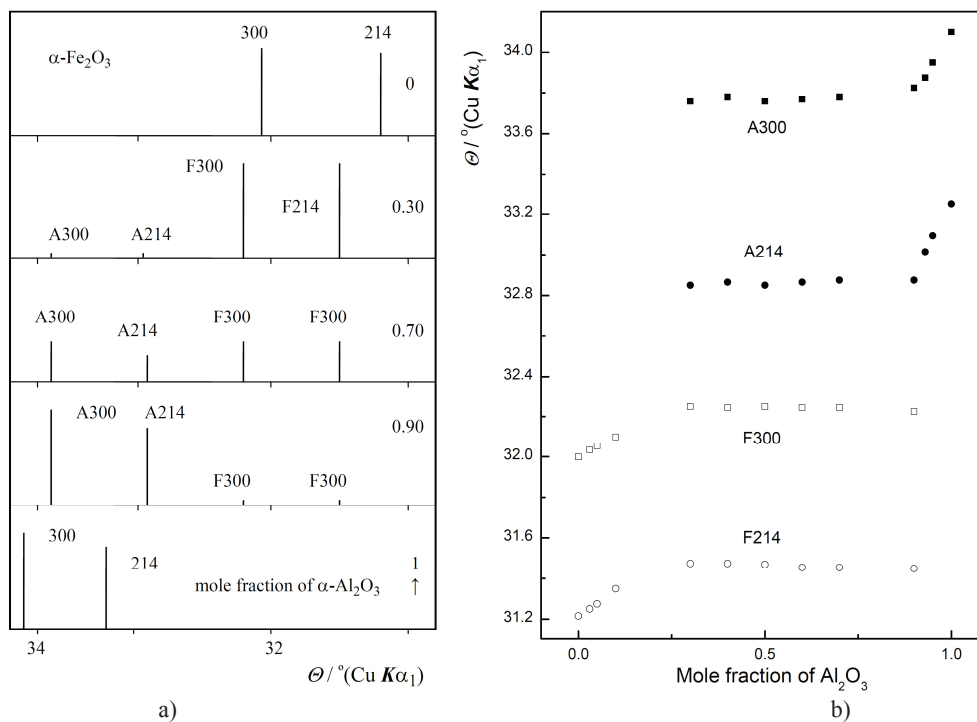
Sample	Mole fraction of Al_2O_3	Phase composition (approx. mole fractions)
AF1	0.03	F
AF2	0.05	F
AF3	0.10	F
AF4	0.30	F + A (0.05)
AF5	0.40	F + A (0.22)
AF6	0.50	F + A (0.37)
AF7	0.60	A + F (0.47)
AF8	0.70	A + F (0.32)
AF9	0.90	A + F (0.01)
AF10	0.93	A
AF11	0.95	A
AF0	1	A

whereas the fraction of the F phase decreased and the fraction of the A phase increased as x increased. All samples exhibited sharp X-ray diffraction lines for both phases A and F, with well-resolved spectral doublets $K\alpha_1\alpha_2$ at higher Bragg angles. The terminal solubility limits, $r = 27.0 \pm 0.5$ of α-Al_2O_3 in α-Fe_2O_3 and $r = 9.0 \pm 0.5$ mole ratio of α-Fe_2O_3 in α-Al_2O_3, were cal-

culated from the dependence of the diffraction line intensities of both phases A and F on x by extrapolation to zero intensity.

The higher solubility of α-Al_2O_3 into α-Fe_2O_3 may be linked to the fact that Al^{3+} cation is about 20 % smaller than Fe^{3+} cation. The present results clearly indicate that there is no formation of a single solid solution phase in the whole concentration range, $0 \le x \le 1$, for the mixed oxide system α-$(Al_xFe_{1-x})_2O_3$, which would obey the Vegard rule.

Musić *et al.*[17,18] investigated the formation of solid solutions in related mixed oxide systems Fe_2O_3-Ga_2O_3 and Fe_2O_3-Cr_2O_3, while Ristić *et al.*[19] investigated the Fe_2O_3-In_2O_3 system. The samples in the system Fe_2O_3-Ga_2O_3 [17] were obtained by coprecipitation and heating the coprecipitates to 600 °C. The presence of only the α-$(Ga_xFe_{1-x})_2O_3$ phase was detected for compositions with x between 0.01 and 0.90, and a gradual decrease in the unit-cell parameters of α-$(Ga_xFe_{1-x})_2O_3$ with the increase in gallium substitution was measured. The samples in the $(Cr_xFe_{1-x})_2O_3$ system, $0 \le x \le 1$,[18] were prepared by a ceramic procedure consisting of the ball-milling of mixed powders α-Fe_2O_3 and Cr_2O_3 using the agate bowl and balls (99.9 % SiO_2), then pressing into tablets and heating to the maximum temperatures of 900 or 1200 °C, respectively. In the whole concentration region, $0 \le x \le 1$

Figure 1. a) Schematic representation of Bragg angles Θ (Cu $K\alpha$) and relative intensities of diffraction lines 214 and 300 of phases A and F for samples S0 ($x = 0$), S4 ($x = 0.30$), S8 ($x = 0.70$), S9 ($x = 0.90$) and S12 ($x = 1$). b) The variation of Bragg angles (Cu $K\alpha$) of diffraction lines 214 and 300 of phases A and F with x.[14]

two phases were found. One phase, F, $\alpha\text{-}(Cr_xFe_{1-x})_2O_3$, is isostructural with $\alpha\text{-}Fe_2O_3$, while the other phase, C is closely related to Cr_2O_3. Phase F existed in samples heated up to 900 °C, for $0 \leq x \leq 0.95$. Phase C existed from $x \geq 0.27$ to $x = 1$ for samples heated up to 900 °C and from $x \geq 0.65$ to $x = 1$ for samples heated up to 1200 °C. For samples heated up to 900 °C, the solubility limits were $r = 27.5 \pm 0.5$ of Cr_2O_3 in $\alpha\text{-}Fe_2O_3$ and $r = 4.0 \pm 0.5$ of Fe_2O_3 in Cr_2O_3. For samples heated to 1200 °C the diffraction peaks for phases F and C in the two-phase region largely overlapped, so the solubility limits could not be determined accurately as for the previous samples. Samples in the Fe_2O_3-In_2O_3 system[19] were prepared by coprecipitation and thermal treatment of isolated hydroxide coprecipitate. For samples heated to 600 °C, a phase $\alpha\text{-}(Fe_{1-x}In_x)_2O_3$, isostructural with $\alpha\text{-}Fe_2O_3$, exists for $0 \leq x \leq 0.8$, and a phase $C\text{-}(Fe_{1-x}In_x)_2O_3$, isostructural with cubic In_2O_3, exists for $0.3 \leq x \leq 1$. In the two-phase region these two phases are poorly crystallized. An amorphous phase is also observed for $0.3 \leq x \leq 0.7$. For samples heated to 900 °C the two-phase region is wider and exists for $0.1 \leq x \leq 0.8$, with two phases well crystallized. In these samples an amorphous phase is not observed. The ionic radius of In^{3+} (0.092 nm) is significantly greater than the ionic radius of Fe^{3+} ion.

Evidently, the ionic radius plays an important role in the formation of solid solutions in the Fe_2O_3-M_2O_3 (M = Al, Ga, Cr, In) oxide systems. Atkinson *et al.*[20] studied the role of metal ion dopants to the corundum-type oxides $\alpha\text{-}M_2O_3$ (M = Al, Cr, Fe). Divalent metal cations are charge compensated by oxygen vacancies, while tetravalent metal cations are compensated by cation vacancies. When a corundum-type structure is doped with isovalent cations of similar radii, for example Al^{3+}, Ga^{3+}, Fe^{3+} and Cr^{3+}, the formation of real solid solutions is preferred. However, it can be noted that the formation of solid solutions is highly dependent on the conditions prevailing in sample preparation. For that reason, very likely, there are discrepancies between data reported in reference literature.

^{57}Fe Mössbauer Spectroscopy

The ^{57}Fe Mössbauer effect is very dependent on changes in the environment of iron ions. For that reason, Mössbauer spectroscopy was used to investigate the samples prepared in the present work. The results of the Mössbauer effect measurements at 20 °C are summarized in Figures 2 to 5 and Table 2. Mössbauer parameters of commercial $\alpha\text{-}Fe_2O_3$, used as starting chemical, are given in Table 2. Incorporation of Al^{3+} ions into the $\alpha\text{-}Fe_2O_3$ structure caused a broadening of spectral lines and a decrease in hyperfine magnetic field in relation to $\alpha\text{-}Fe_2O_3$. For $x = 0.3$ (sample AF4),
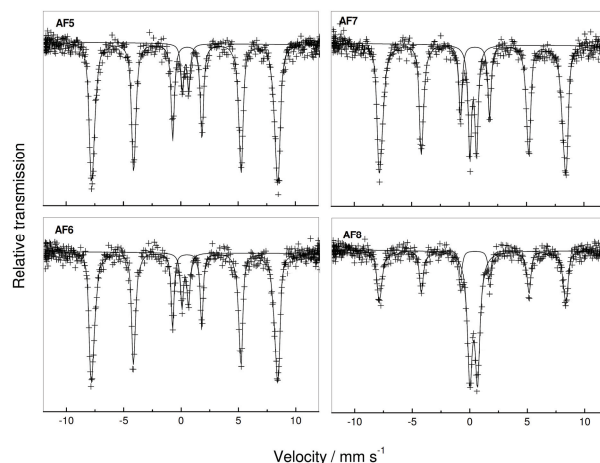
Figure 2. ^{57}Fe Mössbauer spectra of samples AF5 to AF8 at 20 °C.

$\langle B_{hf} \rangle = 49.3$ T was measured. This value was not particularly changed for other samples AF5 through AF8. The Mössbauer spectra of samples AF5 through AF8 are shown in Figure 2, and the corresponding distribution of hyperfine magnetic fields is shown in Figure 3. On the basis of hyperfine magnetic field measurements
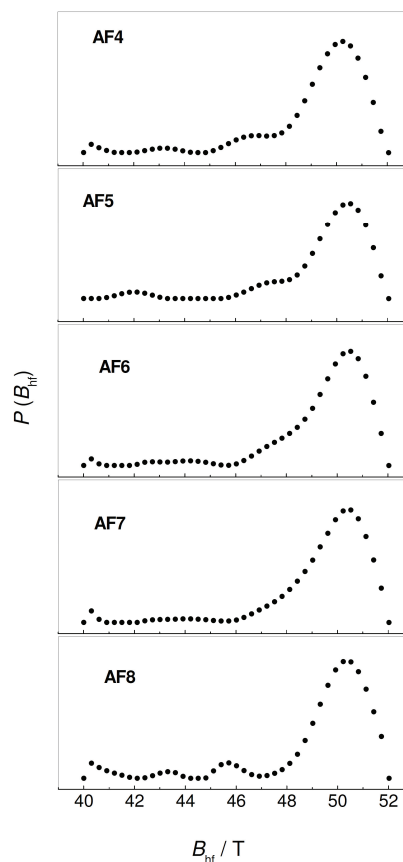
Figure 3. Distribution of hyperfine magnetic fields at 20 °C for samples AF4 to AF8.

Table 2. Calculated Mössbauer parameters at 20 °C

Sample	Spectral line	$\delta^{(a),(b)}$ / mm s^{-1}	$E_Q^{(a)}$ or $2\varepsilon_Q^{(a)}$ / mm s^{-1}	HMF$^{(a)}$ or $\langle B_{hf} \rangle^{(a)}$ / T	Γ / mm s^{-1}	Area / %
Commercial α-Fe₂O₃	M	0.37	-0.21	51.4	0.27	100
AF4	M	0.36	-0.23	49.3$^{(c)}$	0.29	100
AF5	Q	0.35	0.58		0.40	9
	M	0.36	-0.22	49.5$^{(c)}$	0.28	91
AF6	Q	0.35	0.57		0.35	11
	M	0.36	-0.22	49.5$^{(c)}$	0.26	89
AF7	Q	0.35	0.58		0.37	21
	M	0.36	-0.21	49.5$^{(c)}$	0.29	79
AF8	Q	0.34	0.67		0.51	55
	M	0.36	-0.23	49.4$^{(c)}$	0.28	45
AF9	Q1	0.30	0.50		0.29	74
	Q2	0.33	0.69		0.40	26
AF10	Q1	0.30	0.50		0.29	79
	Q2	0.33	0.69		0.37	21
AF11	S	0.03			0.35	7
	Q1	0.29	0.50			74
	Q2	0.33	0.61		0.35	19

$^{(a)}$ Errors: $\delta = \pm 0.01$ mm s^{-1}, ΔE_Q or $2\varepsilon_Q = +0.01$ mm s^{-1}; HMF $= \pm 0.2$ T

$^{(b)}$ Isomer shift, δ, is given relative to α-Fe at 20 °C

$^{(c)}$ Fitted by using the distribution of hyperfine magnetic field ($\langle B_{hf} \rangle$)

for samples AF4 through AF8, it can be concluded that the phase F reached saturation with Al^{3+} ions incorporated in the α-Fe₂O₃ structure. This is in agreement with the XRD results. Figure 2 also shows the presence of central quadrupole doublet(s) in the the Mössbauer spectra of samples AF5 through AF8 where relative intensity is increasing with the increase in the α-Al₂O₃ fraction. Due to simplicity, these spectra were fitted as a superposition of one sextet and one quadrupole doublet. However, Mössbauer spectra recorded for same samples on lower velocity scale showed superposition of two quadrupole doublets. These quadrupole doublets, in accordance with the XRD results, can be assigned to the phase A, *i.e.*, α-Al₂O₃ containing dissolved Fe^{3+} ions. Figure 4 shows the Mössbauer spectra of samples AF9 through AF11. In accordance with its XRD pattern, sample AF9 contains a small fraction of the phase F (estimated at 0.01), while samples AF10 and AF11 contain only the phase A. The spectra of samples AF9 and AF10 were fitted assuming the superposition of two

doublets which indicate two different environments of Fe^{3+} ions in the α-Al₂O₃ structure. However, in the spectrum of sample AF11 a satisfactory fit was obtained by introducing an additional singlet with isomer shift 0.03 mm s^{-1} relative to α-Fe. Brown *et al.*[2] also fitted their Mössbauer spectrum of α-Al₂O₃ doped with $r = 10.5$ Fe₂O₃ for two doublets and one singlet. These authors obtained a near-zero isomer shift of the singlet and relative spectral area close to our case. Their results were interpreted as a nearest-neighbour effect responsible for the appearance of two doublets, whereas the singlet was assigned to the effect of the intermediate phase in the transition aluminas occurring before α-Al₂O₃ crystallization. In the present case the XRD patterns of samples AF10 and AF11 showed only the presence of the α-Al₂O₃ structure. Despite initial differences in sample preparation, the Mössbauer spectra of samples AF9, AF10 and AF11 display a similar phenomenology as in the work by Brown *et al.*[2] Korecz *et al.*[21] recorded the Mössbauer spectrum of Fe^{3+} doped
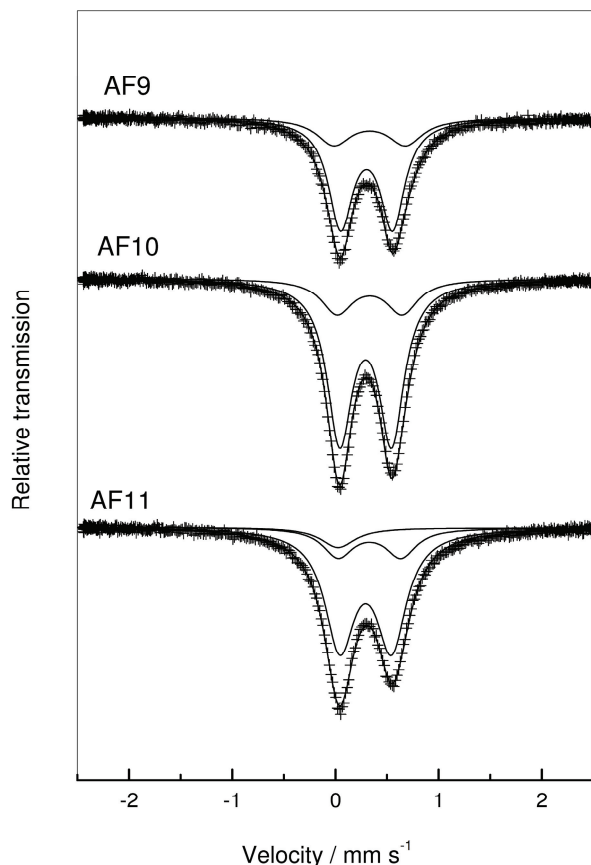
Figure 4. ^{57}Fe Mössbauer spectra of samples AF9 to AF11 at 20 °C.

α-Al$_2$O$_3$ and attributed the quadrupole doublet parameters to the octahedral occupancy in the α-Al$_2$O$_3$ structure. However, it seems that the nature of a singlet in the Mössbauer spectrum of sample AF11 is not fully understood.

FE-SEM

FE-SEM images of selected samples are shown in Figures 5, 6 and 7. The main feature of the samples in their FE-SEM images is a strong sintering effect on the particles. This is understandable because the initial powder was pressed into tablets, then calcined at high temperature. Figure 5a shows a large aggregate belonging to sample AF3. The sintered particles are irregular in shape; however, some of them show hexagonal geometry at the surface. At different optical magnifications (Figure 5bc) the particles of sample AF8 show a better geometrical shape. The dimensions of these particles are also in the μm range and the octahedral nature of these particles is clearly visible. The dimensions of the particles observed for samples AF9, AF10 and AF11 are also in the μm range (Figures 6a, 7). Figure 6b shows EDS of sample AF9. The aluminium and iron content is close to the nominal concentration of these
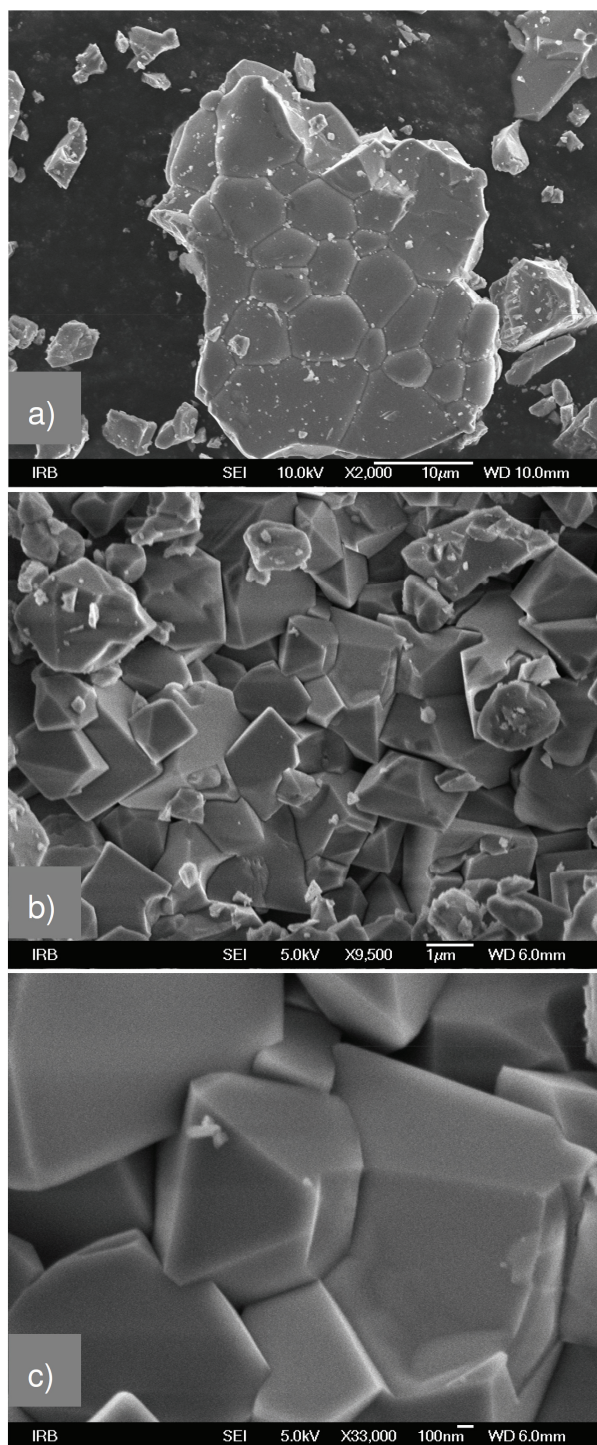

Figure 5. FE-SEM images of (a) sample AF3, and (b,c) sample AF8 at different magnifications.

elements as taken at the start of the preparation procedure. In sample AF9 the mole fraction was $x = 0.99$ for the phase A and $x = 0.01$ for the phase F, as determined by the XRD measurement. Large particles were also observed for samples AF10 and AF11 (Figure 7), however, with rounded edges of their planes.
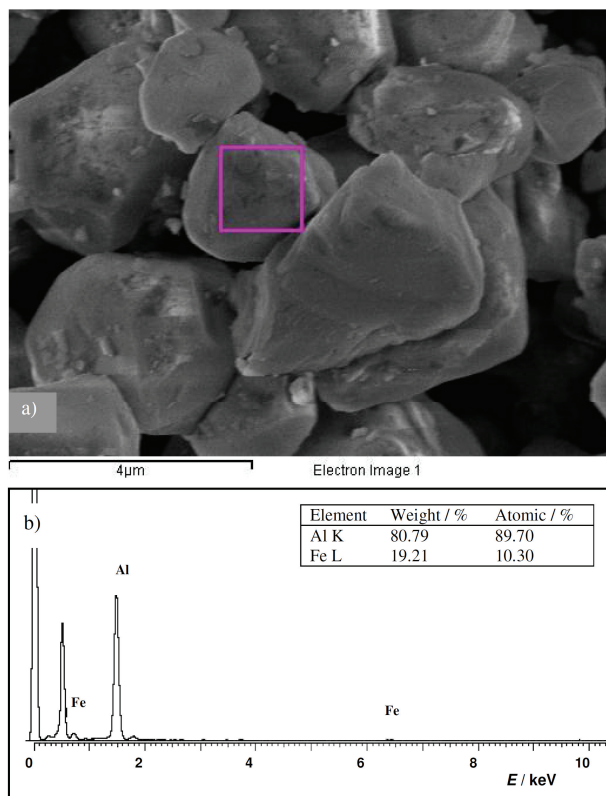
Element	Weight / %	Atomic / %
Al K	80.79	89.70
Fe L	19.21	10.30

Figure 6. FE-SEM image of sample AF9 (a), and EDS of the same sample (b).

CONCLUSION

Two types of solid solutions of the form of $\alpha\text{-}(Al_xFe_{1-x})_2O_3$ were found with XRD: for $0 \leq x \leq 0.91$, the terminal solid solution phase closely related to $\alpha\text{-}Fe_2O_3$, and for $0.27 \leq x \leq 1$, the terminal solid solution phase closely related to $\alpha\text{-}Al_2O_3$.

Incorporation of Al^{3+} ions into the $\alpha\text{-}Fe_2O_3$ structure caused a broadening of Mössbauer lines at 20 °C, and a decrease of the hyperfine magnetic field. In the region $x = 0.40$ to $x = 0.70$ the superposition of the sextet and quadrupole doublet(s) was observed. In this region the hyperfine magnetic field value was nearly constant.

For samples containing $x = 0.93$ and $x = 0.95$ Mössbauer spectra showed the superposition of two quadrupole doublets belonging to two different structural environments of iron ions. With an increase in Al^{3+} content ($x = 0.95$) one singlet with the isomer shift close to zero (relative to $\alpha\text{-}Fe$) was additionally observed; however, its origin is not clearly understood.

A strong sintering effect on the geometrical shape of the particles was observed. Particles were, generally, in the μm dimension range.
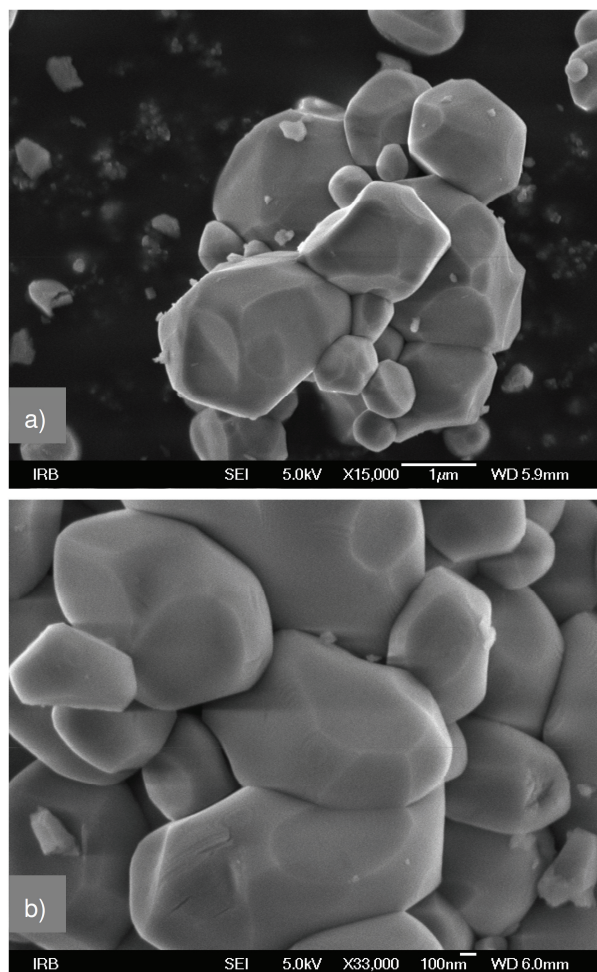

Figure 7. FE-SEM image of (a) sample AF10, and (b) sample AF11.

REFERENCES

1. International Centre for Diffraction Data, Newtown Square, Pa. 19073-3273, USA; Powder Diffraction File, Cards No. 10-173 and 13-534.
2. I. W. M. Brown, K. J. D. MacKenzie, and C. M. Cardile, *J. Mater. Sci. Lett.* **6** (1987) 535–540.
3. E. De Grave, L. H. Bowen, and S. B. Weed, *J. Magn. Magn. Mater.* **27** (1982) 98–108.
4. E. Wolska and W. Szajda, *Solid State Ionics* **28–30** (1988) 1320–1323.
5. A. Cordier, A. Peigney, E. De Grave, E. Flahaut, and C. Laurent, *J. Eur. Ceram. Soc.* **26** (2006) 3099–3111.

6. L. F. Cótica, S. C. Zanatta, M. A. Rocha, I. A. dos Santos, A. Paesano, Jr., J. B. M. da Cunha, and B. Hallouche, *J. Appl. Phys.* **95** (2004) 1307–1314.

7. A. Paesano, Jr., C. K. Matsuda, L. F. Cótica, S. N. de Medeiros, J. B. M. da Cunha, B. Hallouche, and S. L. Silva, *J. Appl. Phys.* **96** (2004) 2540–2546.

8. L. F. Cótica, S. C. Zanatta, S. N. de Medeiros, I. A. dos Santos, A. Paesano, Jr., and J. B. M. da Cunha, *Solid State Ionics* **171** (2004) 283–288.

9. L. F. Cótica, A. Paesano, Jr., S. C. Zanatta, S. N. de Medeiros, and J. B. M. da Cunha, *J. Alloys Compd.* **413** (2006) 265–272.

10. J. Kákoš, L. Bača, P. Veis, and L. Pach, *J. Sol-Gel Sci. Technol.* **21** (2001) 167–172.

11. R. Stösser, M. Nofz, M. Feist, and G. Scholz, *J. Solid State Chem.* **179** (2006) 652–664.

12. M. Liu, H. Li, L. Xiao, W. Yu, Y. Lu, and Z. Zhao, *J. Magn. Magn. Mater.* **294** (2005) 294–297.

13. Z. Y. Zhang. T. Prozorov, I. Felner, and A. Gedanken, *J. Phys. Chem. B* **103** (1999) 947–956.

14. S. Popović, M. Ristić, and S. Musić, *Mater. Lett.* **23** (1995) 139–142.

15. G. Štefanić, S. Musić, and A. Gajović, *Mater. Res. Bull.* **41** (2006) 764–777.

16. G. Štefanić, S. Musić, and A. Gajović, *J. Eur. Ceram. Soc.* **27** (2007) 1001–1016.

17. S. Musić, S. Popović, and M. Ristić, *J. Mater. Sci.* **24** (1989) 2722–2726.

18. S. Musić, M. Lenglet, S. Popović, B. Hannoyer, I. Czakó-Nagy, M. Ristić, D. Balzar, and F. Gashi, *J. Mater. Sci.* **31** (1996) 4067–4076.

19. M. Ristić, S. Popović, M. Tonković, and S. Musić, *J. Mater. Sci.* **26** (1991) 4225–4233.

20. K. J. W. Atkinson, R. W. Grimes, M. R. Levy, Z. L. Coull, and T. English, *J. Eur. Ceram. Soc.* **23** (2003) 3059–3070.

21. L. Korecz, I. Kurucz, G. Menczel, M. E. Pappne, E. Pungor, and K. Burger, *Mag. Kem. Fol.* **78** (1972) 508–511; cited *via* Ref. 2.

SAŽETAK

Istraživanje kristalnih faza u sustavu *α*-Fe₂O₃/*α*-Al₂O₃

Mira Ristić,[a] Stanko Popović[b] i Svetozar Musić[a]

[a]*Zavod za kemiju materijala, Institut Ruđer Bošković, p. p. 180, HR-10002 Zagreb, Hrvatska*
[b]*Fizički odsjek, Prirodoslovno-matematički fakultet, Sveučilište u Zagrebu, HR-10002 Zagreb, Hrvatska*

Smjese α-Fe₂O₃ i γ-AlOOH određenih molnih udjela α-Fe₂O₃ i γ-AlOOH homogenizirane su u planetarnom mlinu, prešane u pastile i grijane do 1200 °C. Svi su uzorci karakterizirani difrakcijom X-zraka u prahu (XRD), Mössbauerovom spektroskopijom (MS), visokorezolucijskom pretražnom elektronskom mikroskopijom (FE SEM) i spektroskopijom karakterističnog X-zračenja (EDS). Detektirane su dvije vrste čvrstih otopina opće formule α-(Al$_x$Fe$_{1-x}$)₂O₃; jedna koja je povezana s α-Fe₂O₃ strukturom i druga koja je povezana s α-Al₂O₃ strukturom. Također, određene su granice topljivosti, molni omjer $r = 27.0 \pm 0.5$ za α-Al₂O₃ u α-Fe₂O₃ i $r = 9.0 \pm 0.5$ za α-Fe₂O₃ u α-Al₂O₃. Primjećeno je širenje Mössbauerovih spektralnih linija i smanjenje vrijednosti hiperfinog magnetskog polja (HMF) s povećanjem udjela Al³⁺ iona u strukturi α-Fe₂O₃. Mössbauerovi spektri čvrstih otopina α-(Al$_x$Fe$_{1-x}$)₂O₃ za molne udjele $x = 0.40–0.70$ karakterizirani su preklapanjem seksteta i jednog ili više dubleta. Unutar ovog koncentracijskog područja gotovo se ne mijenjaju vrijednosti HMF. Mössbauerovi spektri uzoraka α-(Al$_x$Fe$_{1-x}$)₂O₃, za $x = 0.90$ i $x = 0.93$ karakterizirani su preklapanjem dva spektralna dubleta, dok se Mössbauerov spektar uzorka α-(Al$_x$Fe$_{1-x}$)₂O₃ za $x = 0.95$ može opisati preklapanjem dva dubleta i jednog singleta. Podrijetlo ovog singleta s vrijednošću isomernog pomaka ($\delta = 0.03$ mms⁻¹) nije potpuno jasno. Pretražnom elektronskom mikroskopijom primjećen je snažan efekt sinteriranja čestica u svim uzorcima unutar istraživanog α-(Al$_x$Fe$_{1-x}$)₂O₃ sustava.